Supporting Information for

Bedload transport fluctuations, flow conditions and disequilibrium ratio at the Swiss Erlenbach stream: results from 27 years of high-resolution temporal measurements

Dieter Rickenmann[1]

[1]Swiss Federal Research Institute WSL, Birmensdorf, 8903, Switzerland

Contents of this file

Text S1

Figures S1 to S13

Text S1. Small and zero transport rates and small discharges (Figures S2 to S8)

In Figure 2 of the main text there is a wider spread of discharges for a given level of bedload transport in period B than in period A, particularly for $Q < 0.5$ m³ s⁻¹. Therefore, the characteristics of small transport rates at small discharges were examined in some more detail for both periods. Here, I consider both Q_{bz} values (which include zero values) and Q_{bM} values, where zero values have been replaced by averaging with neighbouring non-zero values (see section 2.6). When bins are calculated, this generally results in smaller (and relatively more numerous small) Q_{bM} values for period A than for period B, particularly for discharges Q smaller than 1.0 m³ s⁻¹ (Figure 2).

For $Q > 1.0$ m³ s⁻¹, there are relatively few zero Q_{bz} values (1.2 % for period A, and 2.1 % for period B), so I consider here primarily the distribution of small and zero Q_{bz} values and of small Q_{bM} values for both $Q < 1.0$ m³ s⁻¹ and for $Q < 0.5$ m³ s⁻¹. For the subsets with $Q < 1.0$ m³ s⁻¹, there are relatively more zero Q_{bz} values for period A (20.5 %) than for period B (13.5 %), which is also illustrated in Fig. S2. Looking only at the subsets with $Q < 0.5$ m³ s⁻¹, there are 38% more Q values in period A than in period B (Fig. S3), and the proportion of zero Q_{bz} values is much larger in period A with 34 % than in period B with 19% (s. also Fig. S2).

Still considering the sub-datasets with discharges $Q < 0.5$ m³ s⁻¹ only, there are more small Q_{bz} values in period A than in period B for the range of $Q_{bz} <$ approx. 0.2 kg/s (Fig. S4, zero values not visible in log scale). Looking at the distribution of the Q_{bM} values for the same sub-datasets with discharges $Q < 0.5$ m³ s⁻¹, the relatively larger proportion of small values in period A than in period B is more obvious (Fig. S5, zero values indirectly included).

After ordering the data for each period by increasing Q values, I determined the cumulative sums of Q and Q_{bz} values and plotted them against the relative duration of these measurements in the two periods, separately for the two subsets with either $Q < 1.0$ m³ s⁻¹ or $Q > 1.0$ m³ s⁻¹. For the subsets with $Q < 1.0$ m³/s, it is evident that while there were generally larger discharges in period A than in period B, there was nevertheless more bedload transport in period B than in period A (Fig. S6). I argue in the main text that the higher proportion of both zero and small transport rates in period A is due to a lower availability of easily movable sediment particles on the channel bed in period A as compared to period B. For the subsets with $Q > 1.0$ m³ s⁻¹, there were clearly higher discharges in period B than in period A (Fig. S7).

If we compare the distribution of all Q and Q_{bM} values of the entire datasets for both periods, we find that there are more Q values for the range $Q < 1$ m³ s⁻¹ (Fig. S8(a)) and more Q_{bM} values for $Q_{bM} <$ about 0.1 kg s⁻¹ (Fig. S8(b)) for period A than for period B. (On the other hand, for period B there are more values for flows with Q larger than about 1.8 m³ s⁻¹ and Q_{bM} larger than about 10 kg s⁻¹ (Fig. S8)).
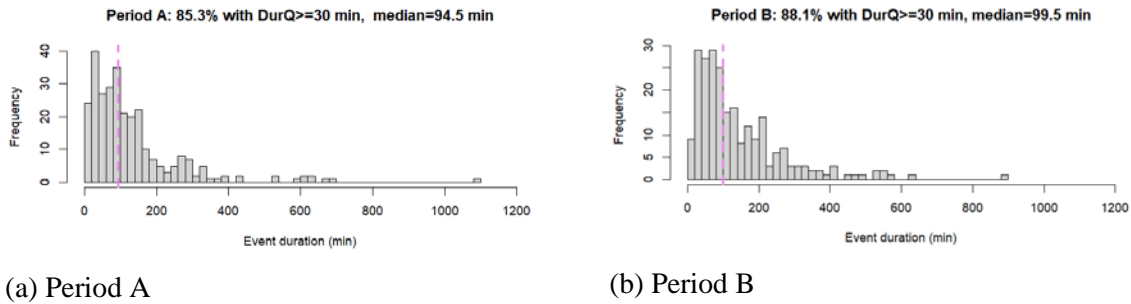
(a) Period A

(b) Period B

Figure S1. Histogram of event durations. (a) for the 286 events of period A and (b) for the 236 events of period B. The vertical dashed pink line indicates the median value.
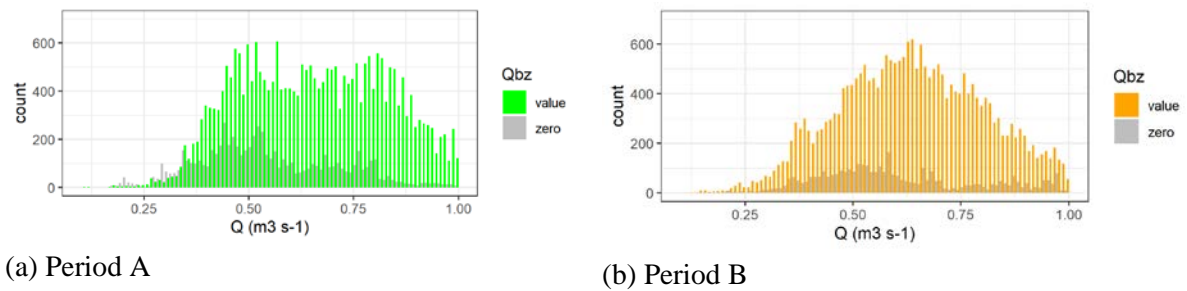
(a) Period A

(b) Period B

Figure S2. Subsets for discharges $Q < 1.0$ m³ s⁻¹. (a) for period A and (b) for period B. There is generally a larger proportion of values with $Q_{bz}=0$ in period A than in period B, for discharges smaller than about 0.8 m³/s. For period A, for Q smaller than about 0.35 m³ s⁻¹, there are generally more zero than non-zero transport values.

(a)

(b)
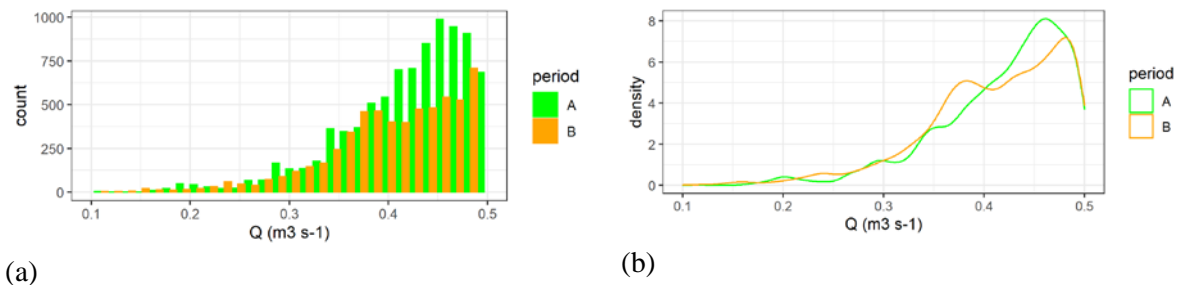
Figure S3. Subsets for discharges $Q < 0.5$ m³ s⁻¹. (a) Histogram and (b) density of Q values.
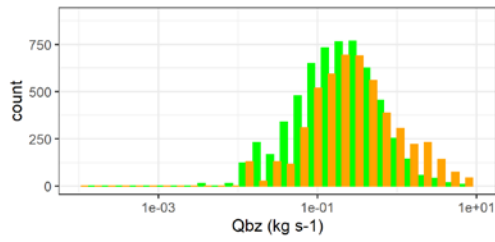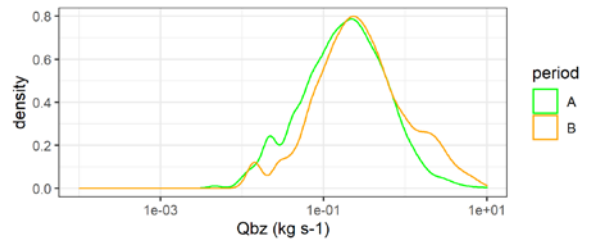
(a) (b)

Figure S4. Subsets for discharges $Q < 0.5$ m^3 s^{-1}. (a) Histogram and (b) Density of Q_{bz} values; note that $Q_{bz} = 0$ values are not shown on log scale.
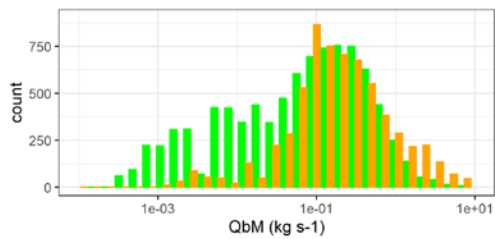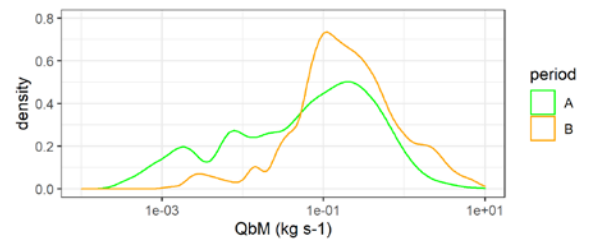
(a) (b)

Figure S5. Subsets for discharges $Q < 0.5$ m^3 s^{-1}. (a) Histogram and (b) density of Q_{bM} values; $Q_{bz} = 0$ values are indirectly included in Q_{bM} values.
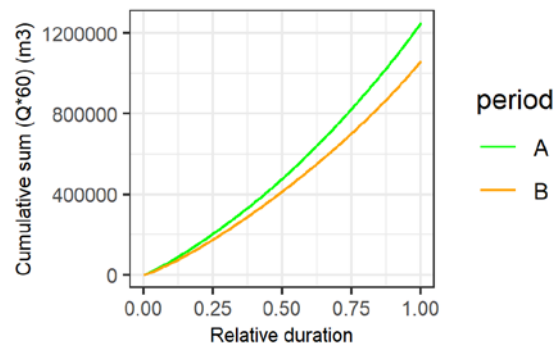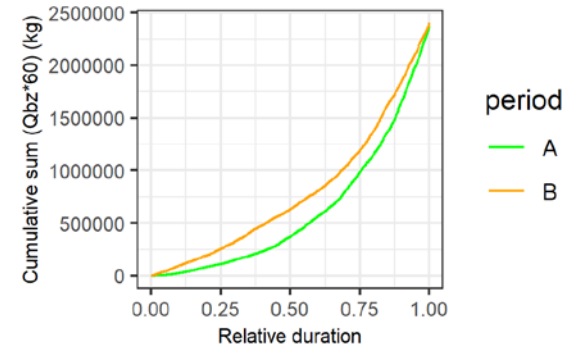
(a) (b)

Figure S6. Subsets for discharges $Q < 1.0$ m^3 s^{-1}. Cumulative sum of (a) Q values and (b) Q_{bz} values, vs. relative duration of these measurements in each period.
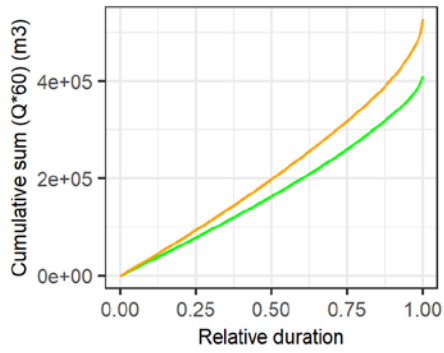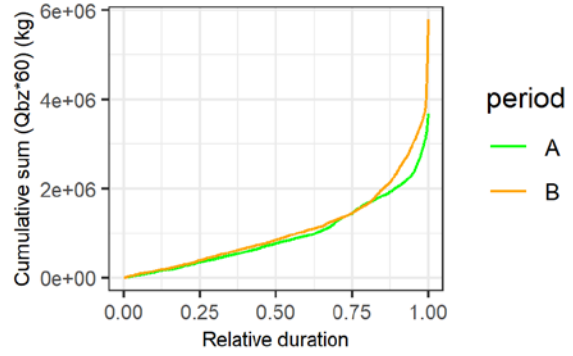
(a)   (b)

Figure S7. Subsets for discharges $Q > 1.0$ m^3 s^{-1}. Cumulative sum of (a) Q values and (b) Q_{bz} values, vs. relative duration of these measurements in each period. The intersection range of the two curves in plot (b) corresponds to a discharge range of 1.7 to 1.8 m^3 s^{-1}.
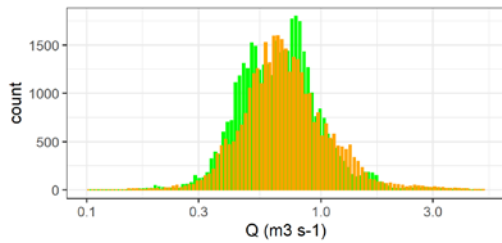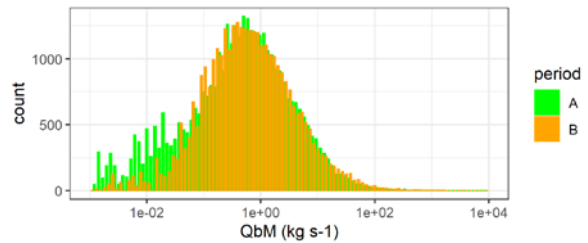
(a)   (b)

Figure S8. Histogram of (a) Q, and (b) Q_{bM} for the entire dataset.
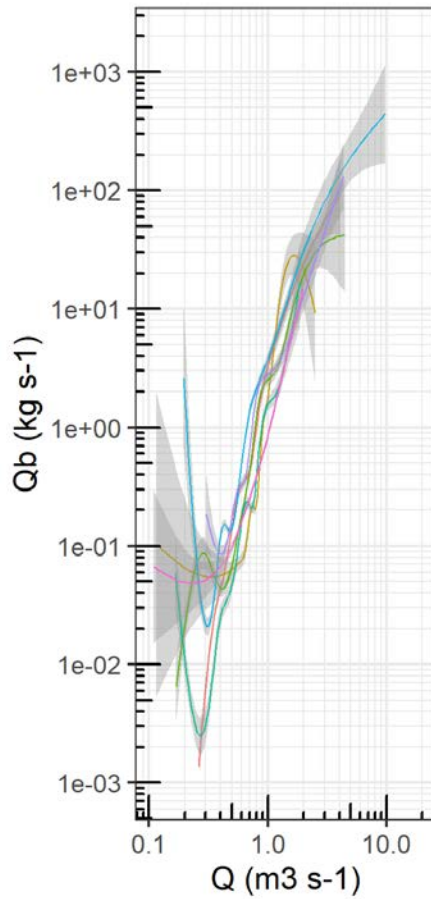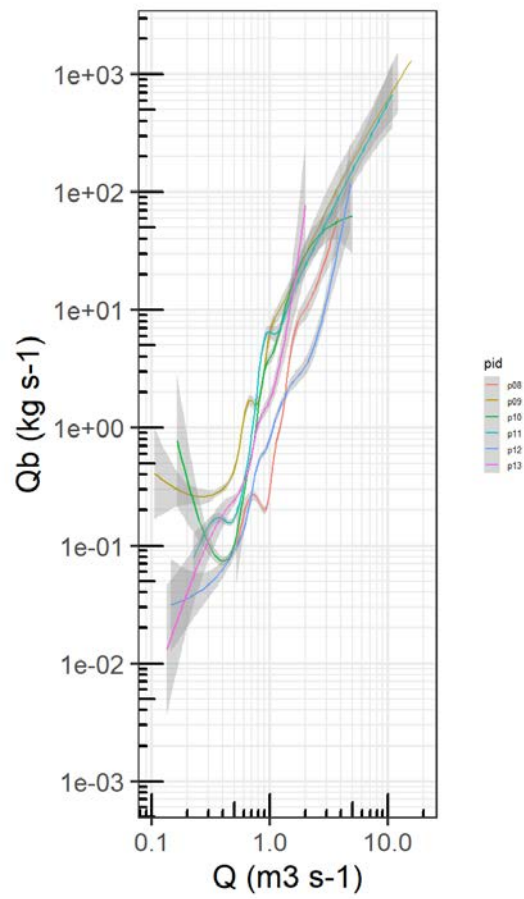
(a)   (b)

Figure S9. Smoothened trend lines for Q_{bM} versus Q were determined separately for the 13 sub-periods of Table 2. (a) period A, and (b) period B. For $Q < 0.5$ m^3 s^{-1} the trend lines are partly horizontal and show no clear increase of Q_{bM} for increasing Q, which is reminiscent of "phase 1" transport conditions (whereby transport rates are relatively low until a certain flow level is reached, Ryan et al., 2002), as is also observed in two Austrian mountain streams with SPG measurements (Rickenmann, 2018). "pid" refers to the number of the sub-periods in Table 2.
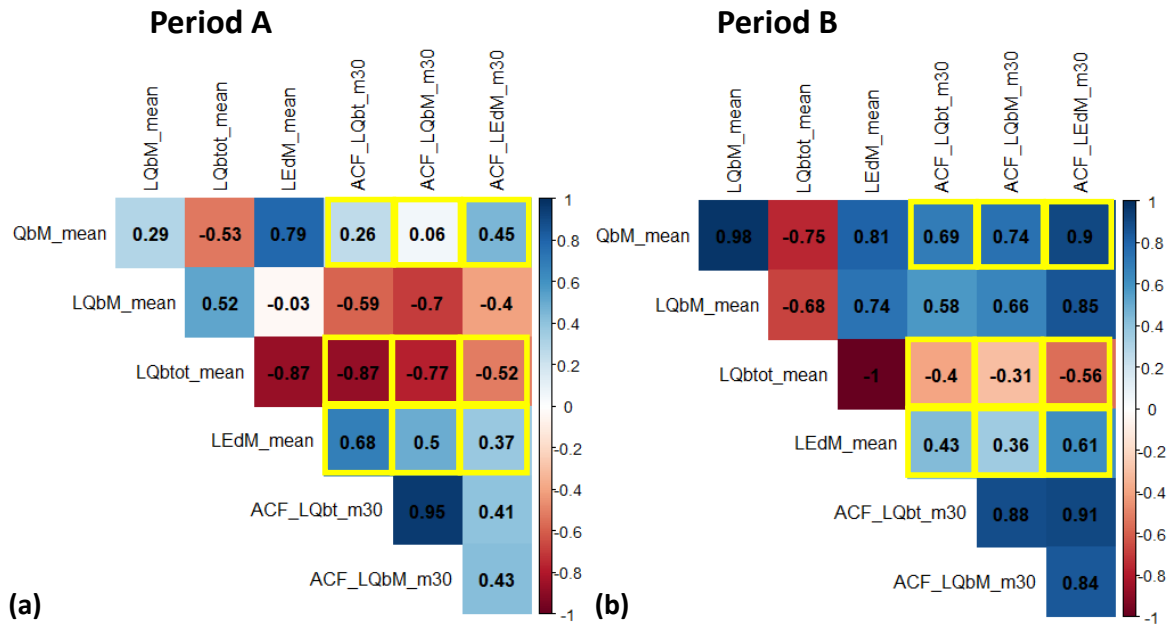
Figure S10. Correlation matrix with Pearson correlation coefficient *R*, for seven variables determined (a) for the 7 sub-periods in period A, and (b) for the 6 sub-periods in period B. The sub-periods are indicated in Figure 5 and Table 2 (main text) for both periods A and B. The fields with a yellow box indicate those variable combinations, for which the correlation has the same sign (positive or negative) when considering the periods A and B together (Fig. 7 in main paper).
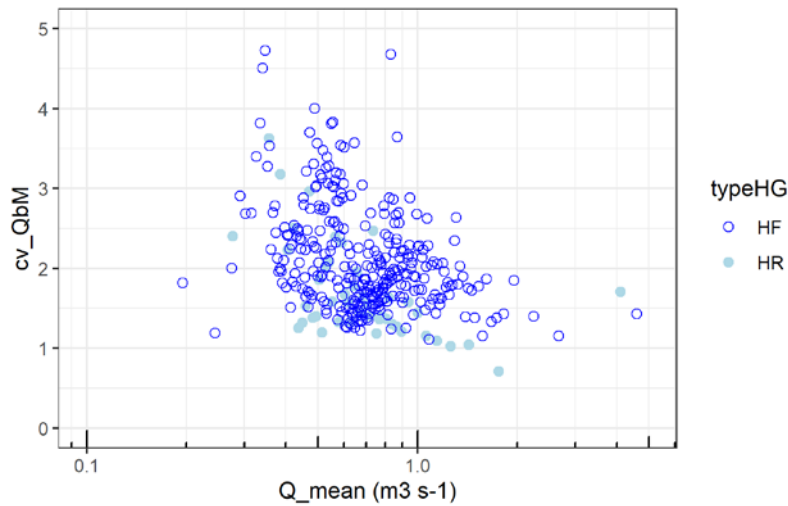
Figure S11. Coefficient of variation of bedload transport rates (cv_Q_{bM}) versus linear mean of discharge (Q_{mean}). The *cv* values were determined separately for the rising (HR) and the falling (HF) limb of the hydrographs, using binned *Q* values, each containing 200 values.

(a)   (b)   (c)
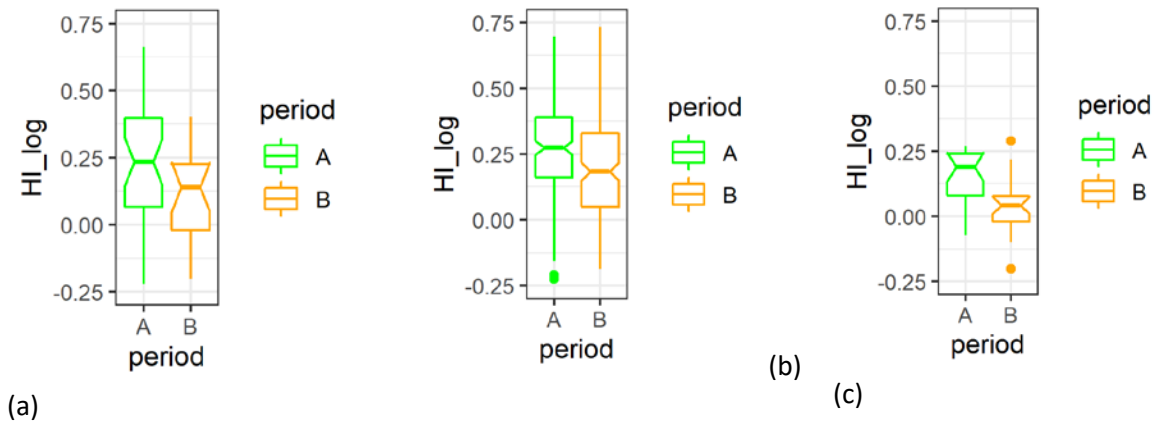
Figure S12. Boxplots of the hysteresis index *HI*_log, determined separately for the three characteristic discharge ranges (S, M, H) of Fig. 3, i.e. for (a) $Q < 0.5$ m^3 s^{-1}, (b) 0.5 m^3 s$^{-1} < Q < 1.8$ m^3 s^{-1}, and (c) $Q > 1.8$ m^3 s^{-1}.
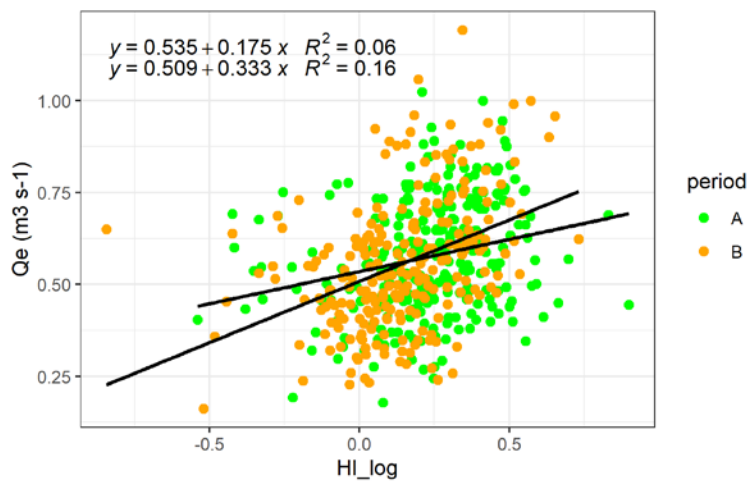
Figure S13. Discharge threshold at the end of an event Q_e versus hysteresis index *HI*_log, determined for each sediment-transporting flood event. The upper linear regression equation (with a flatter slope and smaller R) is for period A, and the lower linear regression equation (with a steeper slope and larger R) is for period B.